Backward Raman amplification of broad-band pulses

A. A. Balakin, I. Y. Dodin, G. M. Fraiman, and N. J. Fisch

Articles you may be interested in

Plasma density measurements using chirped pulse broad-band Raman amplification
Appl. Phys. Lett. **103**, 121106 (2013); 10.1063/1.4821581

Trapping induced nonlinear behavior of backward stimulated Raman scattering in multi-speckled laser beamsa)
Phys. Plasmas **19**, 056304 (2012); 10.1063/1.3694673

Development of a nanosecond-laser-pumped Raman amplifier for short laser pulses in plasma
Phys. Plasmas **16**, 123113 (2009); 10.1063/1.3276739

Envelope-kinetic analysis of the electron kinetic effects on Raman backscatter and Raman backward laser amplification
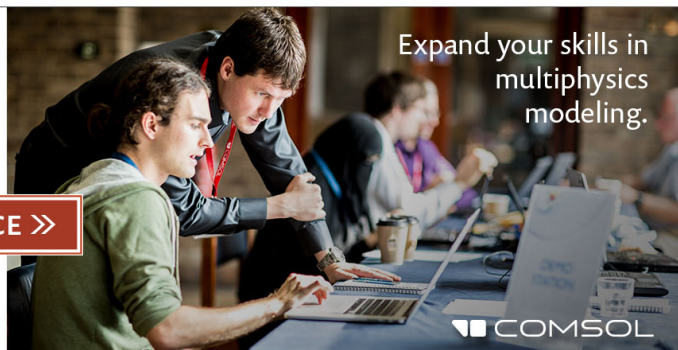Phys. Plasmas **14**, 033104 (2007); 10.1063/1.2646493

Slowly varying envelope kinetic simulations of pulse amplification by Raman backscattering
Phys. Plasmas **11**, 5204 (2004); 10.1063/1.1796351

Backward Raman amplification of broad-band pulses

A. A. Balakin,[1,2] I. Y. Dodin,[3] G. M. Fraiman,[1,2] and N. J. Fisch[3]
[1]Institute of Applied Physics RAS, Nizhny Novgorod, Russia
[2]State University of Nizhny Novgorod, Nizhny Novgorod, Russia
[3]Department of Astrophysical Sciences, Princeton University, Princeton, New Jersey 08544, USA

A reduced fluid model of Raman backscattering is proposed that describes backward Raman amplification (BRA) of pulses with duration τ_0 comparable to or even smaller than the plasma period $2\pi/\omega_p$. At such a small τ_0, a seed pulse can be amplified even if it has the same frequency as the pump (which is technologically advantageous), as opposed to that satisfying the Raman resonance condition. Using our theoretical model, we numerically calculate the BRA efficiency for such pulses as a function of τ_0 and show that it remains reasonably high up to $\tau_0 \approx 2\pi/\omega_p$. We also show that using short seed pulses in BRA makes the amplification less sensitive to quasistatic inhomogeneities of the plasma density. Amplification can persist even when the density perturbations are large enough to violate the commonly known condition of resonant amplification. *Published by AIP Publishing.* [http://dx.doi.org/10.1063/1.4960835]

I. INTRODUCTION

Stimulated Raman backscattering (SRBS) of laser radiation in a plasma is one of the most promising methods of generating short (femtosecond) ultraintense electromagnetic pulses in a laboratory. It is based on the three-wave interaction between a moderately intense yet a long pump wave, a short counterpropagating seed pulse, and Langmuir oscillations excited by the resonant beating of the two. During the SRBS nonlinear stage (i.e., when the pump becomes strongly depleted), the seed shortens while still absorbing most of the pump power; hence, it ends up having intensity much higher than that of the pump. This effect is known as Raman compression or backward Raman amplification (BRA).[1,2]

Due to the large power throughput allowed by a plasma, BRA can, in principle, yield intensities 10^4–10^5 times larger than the conventional chirped-pulse amplification.[3–6] Because of that, the effect has been widely studied recently, including experimentally,[7–9] but building a practical Raman amplifier still requires solving a number of problems. One of such problems is ensuring that the Raman interaction remains resonant over a sufficiently large distance. This requirement is believed to impose strict limitations on the amplitude of plasma density inhomogeneities.[10] Besides, one typically seeks to have the difference between the pump and seed initial frequencies equal to the plasma frequency ω_p, which is not easy to achieve in practice.

Here, we report how these requirements can be relaxed by practicing BRA on extremely short seed pulses. We start by noticing that, if the pulse duration τ_0 is comparable to or smaller than the plasma period $2\pi/\omega_p$, BRA should be possible even if the seed initial frequency ω_{b0} equals that of the pump, ω_{a0}, which case is technologically advantageous. For Brillouin amplification, related experiments were already reported in Refs. 11 and 12, and some theory was discussed in Refs. 13 and 14. For BRA, the effect is yet to be analyzed and assessed quantitatively. To do so is the purpose of this paper.

Specifically, we proceed as follows. First, we develop an improved analytical model of SRBS that does *not* assume the traditional requirement $\omega_{b0} \approx \omega_{a0} - \omega_p$. Then, using this model, we numerically compare the case $\omega_{b0} = \omega_{a0}$ with $\omega_{b0} = \omega_{a0} - \omega_p$ in terms of the BRA efficiency and the output amplitude. We demonstrate that these quantities remain reasonably high up to $\tau_0 \approx 2\pi/\omega_p$. We also show that using short seed pulses in BRA makes the amplification less sensitive to quasistatic inhomogeneities of the plasma density. Amplification can persist even when the density perturbations are large enough to violate the commonly known condition of resonant amplification.

The simplicity of our model allows us to state conclusively that the effects we identified in this paper are robustly of hydrodynamic origin. This provides a guidance to how BRA can be optimized, in the future, at the coarse level. Kinetic effects are the next level of complexity, so they can be studied separately.

The paper is organized as follows. In Sec. II, we derive our reduced analytic model of broad-band BRA. In Sec. III, we summarize our main equations. In Sec. IV, we report the results of our numerical simulations based on this model. In Sec. V, we summarize our main results. Some auxiliary calculations are also presented in the Appendix.

II. GENERAL THEORY

In this section, we present a detailed derivation of our theoretical model. This model is a separate result, which can also help extend the SRBS theory (Sec. II D) beyond the context discussed in this paper. However, a reader who is not interested in details of analytic theory can skip this section and proceed directly to Sec. III.

A. Variational formulation

Equations describing SRBS can be conveniently obtained from the least action principle, $\delta S = 0$, where S is

the action integral, $S = \int \mathfrak{L} \, dt \, d^3x$. Assuming that the plasma is cold, the Lagrangian density $\mathfrak{L}$ can be expressed as follows:[15]

$$\mathfrak{L}[\phi, \mathbf{A}, n_s, \theta_s] = \frac{E^2 - B^2}{8\pi} - \sum_s n_s[\partial_t \theta_s + H_s(t, \mathbf{x}, \nabla\theta_s)].$$
(1)

Here, $\mathbf{E} = -\nabla\phi - \partial_\tau \mathbf{A}$ and $\mathbf{B} = \nabla \times \mathbf{A}$ are the electric and magnetic fields, and ϕ and $\mathbf{A}$ are the scalar and vector potentials, correspondingly; $\tau \doteq ct$ (we use $\doteq$ to denote definitions), and c is the speed of light. The sum is taken over all species, n_s are the corresponding densities, and H_s are the corresponding Hamiltonians; specifically,

$$H_s(t, \mathbf{x}, \nabla\theta_s) = e_s\phi(t, \mathbf{x}) + \sqrt{m_s^2 c^4 + [c\nabla\theta_s - q_s\mathbf{A}(t, \mathbf{x})]^2}.$$
(2)

Here, q_s and m_s are the particle charge and mass, and $\theta_s(t, \mathbf{x})$ is defined such that $\mathcal{P}_s \doteq \nabla\theta_s$ is the canonical momentum of the sth fluid.

We assume that the interaction occurs mostly along some axis z and adopt $\mathbf{A} \approx \mathbf{A}_\perp$, so $E_z \approx -\partial_z\phi$. We will allow for small corrections due to diffraction, but other than that, transverse gradients will be considered negligible. Hence, we assume $\nabla\theta_s \approx \mathbf{e}_z\partial_z\theta_s(t, z)$, where $\mathbf{e}_z$ is the unit vector along z axis. This implies that $\mathcal{P}_{s,\perp}$ is conserved, or, more precisely, equal to zero, since the plasma is initially at rest. (Note also that $p_{z,s} \doteq \partial_z\theta_s$ are the z-projections of the kinetic momenta.) Then, the electron Hamiltonian can be written as follows:

$$H_e = q_e\phi + \sqrt{m_e^2 c^4 + (c\,\partial_z\theta_e)^2 + q_e^2 A_\perp^2}.$$
(3)

We assume ions to be approximately motionless due to large enough m_i. Then,

$$H_i = q_i\phi + m_i c^2 + O(m_i^{-1}) \approx q_i\phi + m_i c^2.$$
(4)

Assuming that the plasma is initially neutral and has electron density $n_0(\mathbf{x})$, we also get $\sum_i (qn)_i = -q_e n_0$, where the sum is taken over ions only, and $q_e \equiv -e < 0$ is the electron charge. We will also assume that $n_0(\mathbf{x}) \sim \bar{n}$ at all $\mathbf{x}$, where $\bar{n}$ is some constant characteristic density. (A more specific definition of $\bar{n}$ will not be necessary.)

Let us now combine the above formulas and drop the constant terms $\int (nmc^2)_s \, dt \, d^3x$ and $\int \partial_t(n\theta)_i \, dt \, d^3x$. After omitting the index e for brevity, we obtain

$$\mathfrak{L} = \mathfrak{L}_{em} + \mathfrak{L}_\phi + \mathfrak{L}_{kin},$$
(5)

$$\mathfrak{L}_{em} = \frac{(\partial_\tau \mathbf{A}_\perp)^2}{8\pi} - \frac{(\nabla \times \mathbf{A}_\perp)^2}{8\pi},$$
(6)

$$\mathfrak{L}_\phi = \frac{(\partial_z\phi)^2}{8\pi} + e(n - n_0)\phi,$$

$$\mathfrak{L}_{kin} = -n\left[\partial_t\theta + mc^2\sqrt{1 + \frac{(\partial_z\theta)^2}{m^2 c^2} + \frac{e^2 A_\perp^2}{m^2 c^4}} - mc^2\right].$$
(7)

Although we will not use the Euler-Lagrange equations (ELEs) that flow from this Lagrangian density directly, we present these equations for completeness

$$\delta\mathbf{A}_\perp: \quad \partial_t^2\mathbf{A}_\perp - c^2\nabla^2\mathbf{A}_\perp = -(4\pi ne^2/m\gamma)\,\mathbf{A}_\perp, \quad (8)$$

$$\delta\theta: \quad \partial_t n + \partial_z(np_z/m\gamma) = 0, \quad (9)$$

$$\delta n: \quad \partial_t p_z + \partial_z(mc^2\gamma - e\phi) = 0, \quad (10)$$

$$\delta\phi: \quad \nabla^2\phi = 4\pi e(n - n_0). \quad (11)$$

Here and further, the notation "δx": means that the corresponding equation is obtained by extremizing the action integral with respect to x. [More strictly speaking, Eq. (10) was obtained by applying ∂_z to the corresponding ELE.] Also, γ is the instantaneous Lorentz factor

$$\gamma \doteq \sqrt{1 + \frac{p_z^2}{m^2 c^2} + \frac{e^2 A_\perp^2}{m^2 c^4}}.$$
(12)

Also notably, one could, in principle, replace a real vector equation (8) with an equation for a complex scalar, say, $A_c \doteq A_x + iA_y$, and express γ through $|A_c|^2$.

B. Field spectrum

Consider the electromagnetic field using its spectral representation, namely,

$$\mathbf{A}_\perp(t, z) = \int_{-\infty}^{\infty} \int_{-\infty}^{\infty} \mathcal{A}(\omega, k)e^{-i\omega t + ikz} \, d\omega \, dk. \quad (13)$$

We will assume that $\mathcal{A}(\omega, k)$ is peaked around some characteristic wave numbers $\pm k_0$. We will also assume that the plasma is dilute, meaning that the characteristic plasma frequency $\bar{\omega}_p \doteq (4\pi\bar{n}e^2/m)^{1/2}$ is much smaller than the characteristic frequency of the electromagnetic field, ω_0; hence, $k_0 \approx \omega_0/c$. (Still, $k_0 - \omega_0/c$ will be considered nonzero.) We will also assume that the width of the spectral peaks, Δk, is sufficiently narrow compared to $2k_0$ yet possibly comparable to, or even larger than, $\bar{\omega}_p/c$. This is summarized as follows:

$$\frac{2\omega_0}{c} \approx 2k_0 \gg \Delta k \sim \frac{\bar{\omega}_p}{c}. \quad (14)$$

Hence, the spectrum $\mathcal{A}(\omega, k)$ can be split into four localized components

$$\mathcal{A} = \mathcal{A}_a + \mathcal{A}_a^* + \mathcal{A}_b + \mathcal{A}_b^*, \quad (15)$$

where $\mathcal{A}_a(\omega, k)$ is peaked at (ω_0, k_0) and $\mathcal{A}_b$ is peaked at $(\omega_0, -k_0)$. Hence, we decompose the vector potential as $\mathbf{A}_\perp = \mathbf{A}_a + \mathbf{A}_a^* + \mathbf{A}_b + \mathbf{A}_b^*$, where

$$\mathbf{A}_{a,b} \doteq \int_{-\infty}^{\infty} \int_{-\infty}^{\infty} \mathcal{A}_{a,b}(\omega, k)e^{-i\omega t + ikz} \, d\omega \, dk \quad (16)$$

are complex fields. The term $\mathbf{A}_a + \mathbf{A}_a^*$ describes waves propagating in the $+z$ direction and is identified as a pump wave.

The term $\mathbf{A}_b + \mathbf{A}_b^*$ describes waves propagating in the $-z$ direction and is identified as a seed wave.

Let us also introduce the following dimensionless fields:

$$\boldsymbol{\alpha} \doteq \frac{e\mathbf{A}_\perp}{mc^2}, \quad \mathbf{a} \doteq \frac{e\mathbf{A}_a}{mc^2}, \quad \mathbf{b} \doteq \frac{e\mathbf{A}_b}{mc^2}, \tag{17}$$

so $\boldsymbol{\alpha} = \mathbf{a} + \mathbf{a}^* + \mathbf{b} + \mathbf{b}^*$.[16] (Keep in mind that, while $\mathbf{a}$ and $\mathbf{b}$ are complex, $\boldsymbol{\alpha}$ is real.) Then

$$\mathfrak{L}_{em} = \frac{m^2 c^4}{8\pi e^2}[(\partial_\tau \boldsymbol{\alpha})^2 - (\nabla \times \boldsymbol{\alpha})^2]. \tag{18}$$

After omitting the rapidly oscillating terms, which are insignificant, one can also reduce this expression to

$$\mathfrak{L}_{em} = \frac{m^2 c^4}{8\pi e^2}\left(|\partial_\tau \mathbf{a}|^2 + |\partial_\tau \mathbf{b}|^2 - |\nabla \times \mathbf{a}|^2 - |\nabla \times \mathbf{b}|^2\right).$$

C. Approximate Lagrangian density

In this paper, we limit our consideration to nonrelativistic intensities ($\alpha \ll 1$). Then, $\mathfrak{L}_{kin}$ can be Taylor-expanded as follows:

$$\mathfrak{L}_{kin} = -n\left[\partial_t \theta + \frac{(\partial_z \theta)^2}{2m} + U\right], \tag{19}$$

where $U \doteq mc^2 \alpha^2/2$ serves as an effective potential. More specifically, one obtains

$$U = mc^2(|\mathbf{a}|^2 + |\mathbf{b}|^2 + \mathbf{a}\cdot\mathbf{b}^* + \mathbf{a}^*\cdot\mathbf{b})$$
$$+ \frac{mc^2}{2}(a^2 + a^{*2} + \mathbf{a}\cdot\mathbf{b} + \mathbf{a}^*\cdot\mathbf{b}^* + b^2 + b^{*2}).$$

Since $a, b \sim \exp(\pm ik_0 z)$, the electron density n and phase θ will respond to this effective potential U at spatial harmonics $k \sim 0, \pm 2k$. Hence, we represent them as follows:

$$n = \bar{n}(N + f + f^*), \quad \theta = \Theta + \tilde{\theta} + \tilde{\theta}^*. \tag{20}$$

Here, N and Θ have slow spatial dependence compared to f and $\tilde{\theta}$. Regarding their temporal dependence, we expect f and $\tilde{\theta}$ to evolve with frequencies *of the order* of $\bar{\omega}_p \ll \omega$, but we do not require these fields to be quasimonochromatic in time.

Equation (19) can now be expressed as

$$\mathfrak{L}_{kin} = -\bar{n}(N + f + f^*)\left[\partial_t \Theta + \partial_t \tilde{\theta} + \partial_t \tilde{\theta}^*\right.$$
$$+ \frac{(\partial_z \Theta)^2}{2m} + \frac{\partial_z \Theta}{m}(\partial_z \tilde{\theta} + \partial_z \tilde{\theta}^*) + \frac{|\partial_z \tilde{\theta}|^2}{m}$$
$$\left. + mc^2(|\mathbf{a}|^2 + |\mathbf{b}|^2 + \mathbf{a}\cdot\mathbf{b}^* + \mathbf{a}^*\cdot\mathbf{b}) + \tilde{H}\right], \tag{21}$$

where

$$\tilde{H} \doteq \frac{1}{2m}\left(\partial_z \tilde{\theta}^2 + \partial_z \tilde{\theta}^{*2}\right) + \frac{mc^2}{2}(a^2 + a^{*2} + \mathbf{a}\cdot\mathbf{b}$$
$$+ \mathbf{a}^*\cdot\mathbf{b}^* + b^2 + b^{*2}).$$

Since all terms in $n\tilde{H}$ oscillate rapidly either in time or in space, this term can be omitted. The same applies to other nonresonant terms. This leads to an equivalent Lagrangian density

$$\mathfrak{L}_{kin} = -\bar{n}N\left[\partial_t \Theta + \frac{(\partial_z \Theta)^2}{2m} + \frac{|\partial_z \tilde{\theta}|^2}{m}\right.$$
$$\left. + mc^2(|\mathbf{a}|^2 + |\mathbf{b}|^2)\right] + \mathfrak{L}_R + \mathfrak{L}_R^*, \tag{22}$$

where $\mathfrak{L}_R$ is given by

$$\mathfrak{L}_R \doteq -\bar{n}f\left[\partial_t \tilde{\theta}^* + \frac{1}{m}(\partial_z \Theta)(\partial_z \tilde{\theta}^*) + mc^2(\mathbf{a}^*\cdot\mathbf{b})\right].$$

Let us also represent the scalar potential as

$$\phi = \frac{mc^2}{e}\left(\Phi + \tilde{\phi} + \tilde{\phi}^*\right), \tag{23}$$

where Φ is slow compared to $\tilde{\phi} \sim \exp(2ik_0 z)$; hence,

$$\mathfrak{L}_\phi = \frac{m^2 c^4}{8\pi e^2}\left[(\partial_z \Phi)^2 + 2|\partial_z \tilde{\phi}|^2\right]$$
$$+ mc^2 \bar{n}(N - N_0)\Phi + mc^2 \bar{n}\left(f\tilde{\phi}^* + f^*\tilde{\phi}\right), \tag{24}$$

where $N_0 \doteq n_0/\bar{n}$. The full Lagrangian density (5) is then cast as follows:

$$\mathfrak{L} = mc^2 \bar{n}(N - N_0)\Phi + mc^2 \bar{n}\left(f\tilde{\phi}^* + f^*\tilde{\phi}\right)$$
$$+ \frac{m^2 c^4}{8\pi e^2}\left[(\partial_z \Phi)^2 + 2|\partial_z \tilde{\phi}|^2\right]$$
$$+ \frac{m^2 c^4}{8\pi e^2}\left[(\partial_\tau \mathbf{a})^2 + (\partial_\tau \mathbf{b})^2 - (\nabla \times \mathbf{a})^2 - (\nabla \times \mathbf{b})^2\right]$$
$$- \left[\partial_t \Theta + \frac{(\partial_z \Theta)^2}{2m} + \frac{|\partial_z \tilde{\theta}|^2}{m} + mc^2(|\mathbf{a}|^2 + |\mathbf{b}|^2)\right]\bar{n}N$$
$$- \left[\partial_t \tilde{\theta}^* + \frac{1}{m}(\partial_z \Theta)(\partial_z \tilde{\theta}^*) + mc^2 \mathbf{a}^*\cdot\mathbf{b}\right]\bar{n}f$$
$$- \left[\partial_t \tilde{\theta} + \frac{1}{m}(\partial_z \Theta)(\partial_z \tilde{\theta}) + mc^2 \mathbf{a}\cdot\mathbf{b}^*\right]\bar{n}f^*. \tag{25}$$

D. Dimensionless equations

Let us measure $\mathfrak{L}$ in units $mc^2 \bar{n}$, time in units ω_0^{-1}, coordinates in units c/ω_0, and θ and $\tilde{\theta}$ in units mc^2/ω_0. Let us also introduce

$$\beta \doteq \bar{\omega}_p^2/\omega_0^2 \ll 1. \tag{26}$$

Hence, Eq. (25) can be cast as follows:

$$\mathfrak{L} = (N - N_0)\Phi + f\tilde{\phi}^* + f^*\tilde{\phi}$$
$$+ \frac{1}{2\beta}\left[(\partial_z\Phi)^2 + 2|\partial_z\tilde{\phi}|^2\right]$$
$$+ \frac{1}{2\beta}\left[(\partial_t\mathbf{a})^2 + (\partial_t\mathbf{b})^2 - (\nabla \times \mathbf{a})^2 - (\nabla \times \mathbf{b})^2\right]$$
$$- \left[\partial_t\Theta + \frac{(\partial_z\Theta)^2}{2} + \Psi\right]N$$
$$- \left[\partial_t\tilde{\theta}^* + (\partial_z\Theta)(\partial_z\tilde{\theta}^*) + \mathbf{a}^* \cdot \mathbf{b}\right]f$$
$$- \left[\partial_t\tilde{\theta} + (\partial_z\Theta)(\partial_z\tilde{\theta}) + \mathbf{a} \cdot \mathbf{b}^*\right]f^*, \qquad (27)$$

where $\Psi \doteq |\partial_z\tilde{\theta}|^2 + |\mathbf{a}|^2 + |\mathbf{b}|^2$ is the ponderomotive potential. Since the seed pulse is expected to quickly grow larger than the pump wave, $\Psi \approx |\mathbf{b}|^2$ is typically a good approximation for Ψ. Nevertheless, retaining the complete expression for Ψ in the Lagrangian density is necessary to obtain the correct equations for f and $\mathbf{a}$.

The ELEs corresponding to the above Lagrangian density are as follows:

$$\delta\mathbf{b}^*: \quad (\partial_z^2 - \partial_t^2)\mathbf{b} = \beta(N\mathbf{a} + \mathbf{a}f^*) - \nabla_\perp^2\mathbf{b}, \qquad (28)$$

$$\delta\tilde{\theta}^*: \quad \partial_t f + \partial_z(N\tilde{p} + fP) = 0, \qquad (29)$$

$$\delta\Phi^*: \quad \partial_z^2\Phi = \beta(N - N_0), \qquad (30)$$

$$\delta f^*: \quad \partial_t\tilde{p} + \partial_z(P\tilde{p} + \mathbf{a} \cdot \mathbf{b}^* - \tilde{\phi}) = 0, \qquad (31)$$

$$\delta\tilde{\phi}^*: \quad \partial_z^2\tilde{\phi} = \beta f, \qquad (32)$$

$$\delta N: \quad \partial_t P + \partial_z(P^2/2 + \Psi - \Phi) = 0, \qquad (33)$$

$$\delta\Theta: \quad \partial_t N + \partial_z(NP + f\tilde{p}^* + f^*\tilde{p}) = 0, \qquad (34)$$

where $P \doteq \partial_z\Theta$ and $\tilde{p} \doteq \partial_z\tilde{\theta}$. Notably, since these are exact ELEs corresponding to the Lagrangian density $\mathfrak{L}$, they remain exactly conservative even though $\mathfrak{L}$ itself is approximate. In particular, such ELEs are automatically applicable to inhomogeneous and even nonstationary plasmas, which otherwise can be tricky to deal with.[17,18] Another advantage of the Lagrangian formulation is that it can be readily extended to account for complex nonlinear effects such as effects of trapped particles. See Refs. [19–21] for how to modify the expression for U in this case, at least for long enough pulses.

E. Neglecting quasistatic fields

The above equations can be simplified further as follows. Assuming that the low-frequency dynamics is determined primarily by the seed pulse, we can take $\partial_t \approx \partial_z$ in all equations for the "slow" variables. Then, from the momentum equation, we have

$$P \approx -P^2/2 - \Psi + \Phi \approx -\Psi + \Phi, \qquad (35)$$

where we made use of the assumption $P \ll 1$. Similarly, from the continuity equation, we have

$$N \approx N_0(1 + P)^{-1} \approx N_0(1 - P) \approx N_0(1 + \Psi - \Phi). \qquad (36)$$

Then, $N - N_0 \approx N_0(\Psi - \Phi)$, so the equation for Φ becomes

$$\partial_z^2\Phi = \beta N_0(\Psi - \Phi). \qquad (37)$$

The above equation predicts two distinct regimes depending on the ratio of the characteristic spatial scale l and $\delta_p \doteq c/\omega_p$. At $l \gg \delta_p$, one has $\partial_z^2 \ll \beta$, so $\Phi \approx \Psi$, which describes an adiabatic response of the plasma to the ponderomotive potential. At $l \lesssim \delta_p$, one has $\Phi \sim \Psi(l/\delta_p)^2$, which describes a wake field. In either case, $\Phi \lesssim \Psi \ll 1$. Since nonrelativistic corrections are neglected in our theory, we must hence adopt $N \approx N_0$. In other words, the effect of all quasistatic fields on the electron density will be neglected.

III. MAIN EQUATIONS

A. Reduced model

To the extent that the plasma density and nonlinearity can be neglected, one has $\partial_t\mathbf{a} \approx -\partial_z\mathbf{a}$ and $\partial_t\mathbf{b} \approx \partial_z\mathbf{b}$, where we used the fact that $\mathbf{a}$ and $\mathbf{b}$ have narrow spectra. Thus, to the first nonvanishing order in $(\partial_t + \partial_z)\mathbf{a}$ and $(\partial_t - \partial_z)\mathbf{b}$, one can write

$$(\partial_z^2 - \partial_t^2)\mathbf{a} \approx 2\partial_z(\partial_t + \partial_z)\mathbf{a}, \qquad (38)$$

$$(\partial_z^2 - \partial_t^2)\mathbf{b} \approx -2\partial_z(\partial_t - \partial_z)\mathbf{b}. \qquad (39)$$

Then, one arrives at the following set of equations:

$$(\partial_t + \partial_z)\mathbf{a} = \hat{K}_a[\beta(N_0\mathbf{a} + \mathbf{b}f) - \nabla_\perp^2\mathbf{a}], \qquad (40)$$

$$(\partial_t - \partial_z)\mathbf{b} = \hat{K}_b[\beta(N_0\mathbf{b} + \mathbf{a}f^*) - \nabla_\perp^2\mathbf{b}], \qquad (41)$$

$$\partial_t f + \partial_z(\tilde{p}N_0) = 0, \qquad (42)$$

$$\partial_t\tilde{p} + \partial_z(\mathbf{a} \cdot \mathbf{b}^*) - \beta\partial_z^{-1}f = 0. \qquad (43)$$

Here, we introduced ∂_z^{-1} as an operator inverse to ∂_z (provided zero boundary conditions, this operator is well defined) and

$$\hat{K}_{a,b} = (\pm 2\partial_z)^{-1}. \qquad (44)$$

Equations (40)–(43) form a new model of SRBS that is one of the main results of this paper. Although we formally required $2k_0 \gg \Delta k$ [Eq. (14)] to derive these equations, we expect that our model can produce reasonably accurate results even for relatively wide electromagnetic spectra, say, with Δk up to $k_0/2$ (because 1/4 is considerably smaller than unity).

Note that our model uses four first-order equations. This makes it different from the traditional three-wave model of SRBS that uses three first-order equations and relies on having the Raman resonance condition[1]

$$\omega_a \approx \omega_b + \omega_p, \qquad (45)$$

where $\omega_{a,b}$ are the carrier frequencies of $\mathbf{a}$ and $\mathbf{b}$, correspondingly, and $\omega_p \doteq \sqrt{4\pi N_0 e^2/m}$ is the local plasma frequency. (The same distinction applies to comparison with other papers, e.g., Refs. [22] and [23], where various modifications of the traditional SRBS model were contemplated but
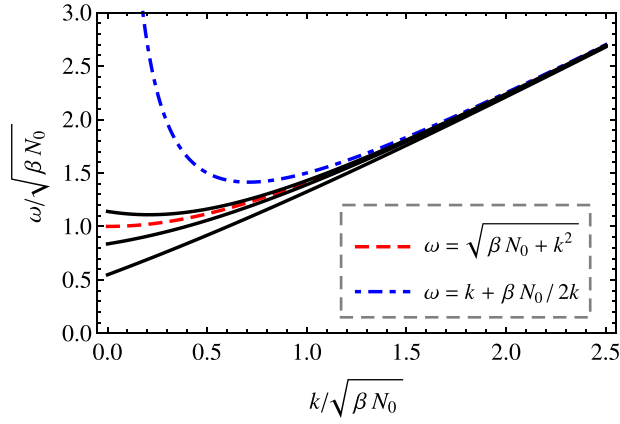
FIG. 1. Comparison of the model dispersion relation (50) (solid black) with the true dispersion relation (46) (red dashed) and the asymptotic dispersion relation (48) (blue dashed). The model dispersion relation is plotted for $N_0 = 0.3, 0.7, 1.3$, where higher curves correspond to larger N_0. It is seen that, at $k \lesssim \sqrt{\beta}$, Eq. (50) is a better approximation of Eq. (46) than Eq. (48). It is also seen that, at $k \gg \sqrt{\beta}$, all three equations predict approximately the same ω.

invariably assumed three-wave resonances at least approximately.) Should the condition (45) be adopted within our model, the equations of Ref. 1 are readily reproduced (see the Appendix).

B. Improved model for $\hat{K}_{a,b}$

For linear plane monochromatic waves in a homogeneous plasma, one expects that harmonics comprising both **a** and **b** satisfy the cold-plasma dispersion relation

$$\omega(k) = \sqrt{\beta N_0 + k^2}. \tag{46}$$

However, from Eqs. (40) and (41), one gets

$$i\partial_t \begin{pmatrix} \mathbf{a} \\ \mathbf{b} \end{pmatrix} = (|k| \mp i\hat{K}_{a,b}) \begin{pmatrix} \mathbf{a} \\ \mathbf{b} \end{pmatrix}. \tag{47}$$

Using Eq. (44), one is hence led to the linear dispersion

$$\omega(k) = |k| + \frac{\beta N_0}{2|k|}. \tag{48}$$

This is the correct asymptotic representation of Eq. (46) for all k of interest, since we have assumed that the electromagnetic energy is mainly concentrated at $|k| \gg \sqrt{\beta}$. However, in simulations, having $\omega(k) \to \infty$ at $k \to 0$ can cause numerical errors to build up. These errors eventually propagate to larger k and then can become a problem. Hence, we propose an alternative model for $\hat{K}_{a,b}$, namely,

$$\hat{K}_{a,b} = -\frac{i}{\sqrt{\beta - \partial_z^2 \mp i\partial_z}}, \tag{49}$$

which corresponds to the linear dispersion

$$\omega(k) = |k| + \frac{\beta N_0}{\sqrt{\beta + k^2} + |k|}. \tag{50}$$

The above equation reproduces the true dispersion relation (46) exactly for $N_0 = 1$ (Ref. 26) and approximates it for arbitrary $N_0 \sim 1$ with fidelity at $|k| \gg \sqrt{\beta}$ (Fig. 1). In other words, replacing Eq. (44) with Eq. (49) bounds the error that
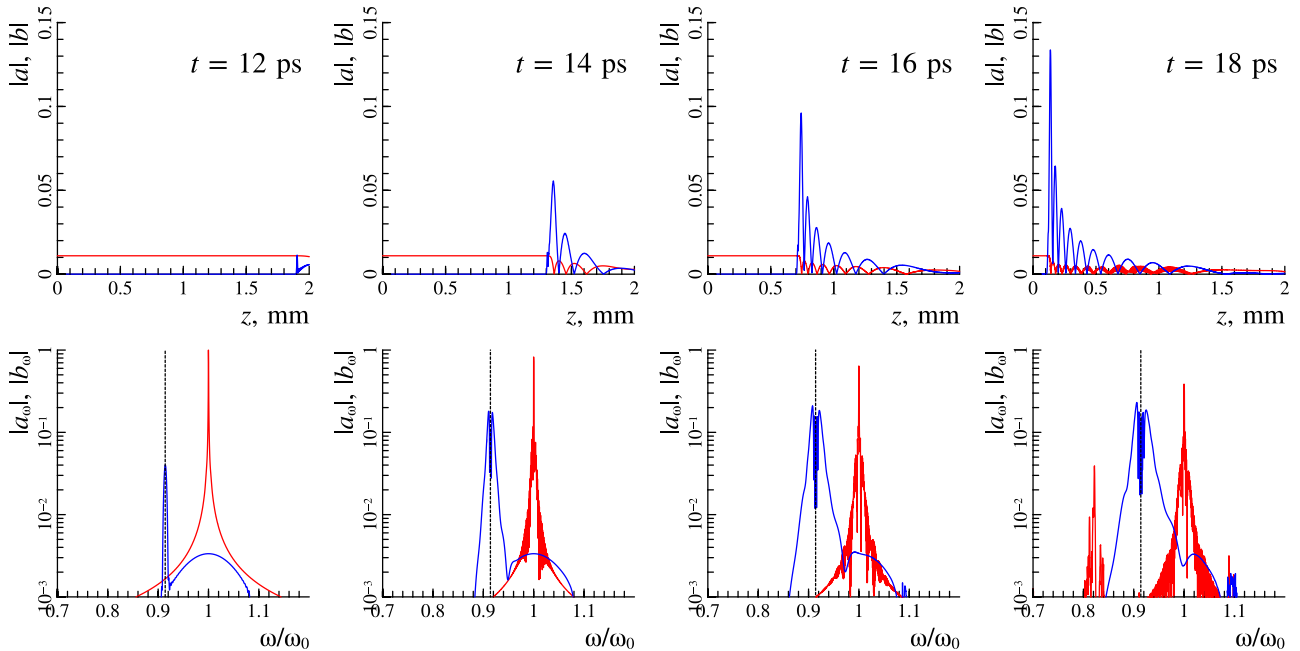

FIG. 2. Sequence of snapshots illustrating the interaction of a linearly polarized pump (red) and seed (blue) with equal carrier frequencies ω_0: upper figures—spatial representation ($|a|$ and $|b|$) and lower figures—spectral representation ($|a_\omega|$ and $|b_\omega|$). The spatial spectra are calculated at the specified moments of time ($t = 12, 14, 16, 18$ ps) and mapped to the frequency domain using Eq. (46). The plasma is homogeneous with density $n_0 = 6 \times 10^{18}$ cm^{-3}, and the assumed wavelength $2\pi c/\omega_0 = 1.053$ μm, so $\omega_p/\omega_0 \approx 0.08$. The initial seed is Gaussian and has the maximum amplitude $b_{max}(t = 0) = 0.01$. The initial pump is step-like (which is why it has a wide spectrum) with the amplitude $a_{max}(t = 0) = 0.01$. In contrast to the traditional three-wave model, the model proposed here captures Raman harmonics at $\omega = \omega_0 - 2\omega_p$ and at $\omega = \omega_0 + \omega_p$, which are seen in the last subfigure. For other relevant aspects of pulse transformation at SRBS, see Refs. 13 and 14.

is caused by adopting Eqs. (38) and (39). Thus, Eq. (49) may be better suited for numerical simulations compared to Eq. (44). This improved model for $\hat{K}_{a,b}$ can be considered as another, secondary distinction between our model and that in Ref. 1.

IV. NUMERICAL RESULTS

As opposed to the traditional three-wave model of SRBS,[1] the model proposed above allows a reduced description of BRA in the regime when the seed pulse has duration

$$\tau_0 \lesssim 2\pi/\omega_p. \tag{51}$$

By integrating Eqs. (40)–(43) numerically [with $\hat{K}_{a,b}$ modeled by Eq. (49)], we show below that using such short pulses in BRA may be advantageous for a number of reasons. For clarity, we focus on the regime when the seed duration is (few) tens of fs and the intensity is comparable to that of the pump. Such pulses are experimentally accessible; for example, see Refs. 24 and 25.

A. Using a seed and a pump with equal carrier frequencies

Since short seed pulses have a broad spectrum, one can anticipate that they can be amplified using SRBS even without the Raman resonance condition (45). Then, the initial seed can be produced using the same laser as the pump without additional frequency transformations, which is technologically advantageous. The above theory allows one to test this idea quantitatively using a simple and robust numerical model.

Our simulations show that efficient BRA (i.e., that with substantial pump depletion) using a seed and a pump with equal initial carrier frequencies (henceforth termed ω_0) is possible indeed. Figure 2 shows a typical evolution of the corresponding fields and their spectra. It is seen that BRA starts in the part of the seed spectrum that is downshifted by ω_p from ω_0. Later, the maximum of the seed spectral amplitude saturates but the *spectrum width* continues to grow, resulting in the increase of the seed maximum amplitude $b_{\max}(t)$. Eventually, a solution similar to the "π pulse"[1] is formed.

The maximum amplitude as a function of τ_0 is shown in Fig. 3(a). In Fig. 3(b), we show the BRA efficiency $\eta \doteq \mathcal{I}_b/\mathcal{I}_a$, where $\mathcal{I}_a \doteq \int |\mathbf{a}|^2 dz$ and $\mathcal{I}_b \doteq \int |\mathbf{b}|^2 dz$ characterize the number of quanta in the pump and seed pulses, respectively. (Having $\eta = 1$ would correspond to complete pump depletion.) For comparison, we also show $b_{\max}$ and η produced at the same plasma parameters but for ω_a and ω_b satisfying Eq. (45). At $\tau_0 \ll 2\pi/\omega_p$, the two schemes produce virtually identical results. But such initial pulses with large enough intensities are harder to prepare,[25] so more realistic is the regime $\tau_0 \sim 2\pi/\omega_p$. In this case, the distinction between the resonant and nonresonant schemes becomes somewhat noticeable, to the extent seen in Fig. 3. Still, the two schemes produce comparable results; i.e., BRA of such short pulses remains possible also without the Raman
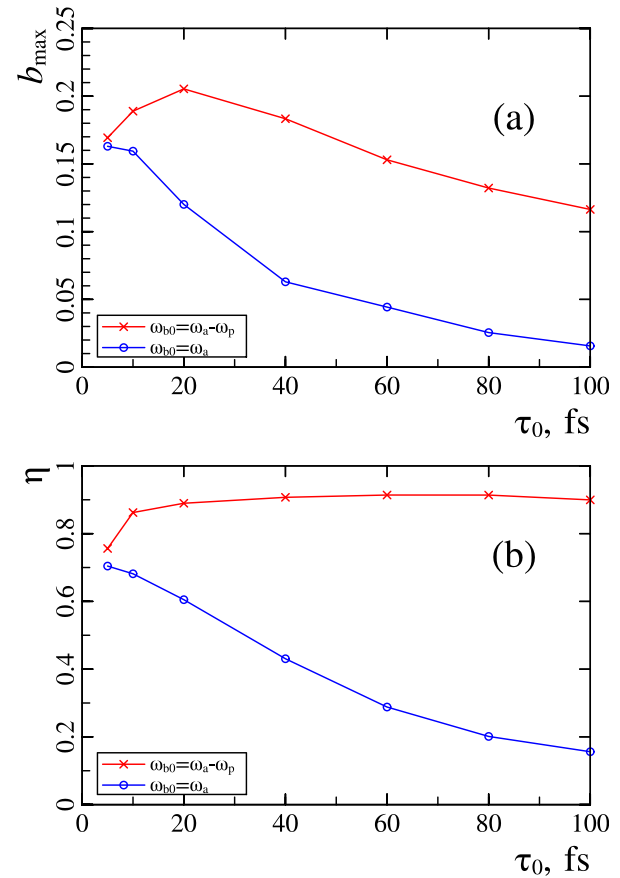

FIG. 3. Comparison of two BRA schemes that use the same carrier frequency of the pump ω_a but different initial carrier frequencies of the seed ω_{b0}: red crosses—$\omega_{b0} = \omega_a - \omega_p$, blue circles—$\omega_{b0} = \omega_a$; τ_0 is the initial seed duration measured in fs. (a) Maximum amplitude of the amplified seed $b_{\max}$ vs τ_0. (b) BRA efficiency η vs τ_0. (Having $\eta = 1$ would correspond to complete pump depletion.) The plasma is 3-mm long and homogeneous otherwise. The other parameters are the same as in Fig. 2; in particular, $2\pi/\omega_p \approx 45$ fs. The initial amplitudes are $a_{\max}(t = 0) = b_{\max}(t = 0) = 0.01$.

resonance condition, as anticipated. At larger τ_0, the efficiency drops, as also expected from findings in Ref. 27.

B. Effect of density inhomogeneities

We also explored numerically how BRA of short pulses is affected by quasistatic inhomogeneities of the plasma density. For simplicity, the electron density was taken in the form

$$N_0 = 1 + \delta N \sin(z/L_\delta) \tag{52}$$

with various amplitudes δN and scales L_δ. The results are shown in Figs. 4 and 5. They indicate that BRA of pulses with τ_0 satisfying Eq. (51) is much less sensitive to inhomogeneities than BRA of longer pulses. [Although the effect of inhomogeneities for short pulses was studied previously in Ref. 10, the extreme regime (51) that we discuss here was not addressed in that paper.] In fact, it is seen that, for a wide range of L_δ, BRA tolerates δN up to unity if the pulse duration is sufficiently small.

This is a nontrivial effect, because it is not anticipated from the traditional theory of resonant BRA. According to Ref. 3, the seed bandwidth is irrelevant (the Green's function
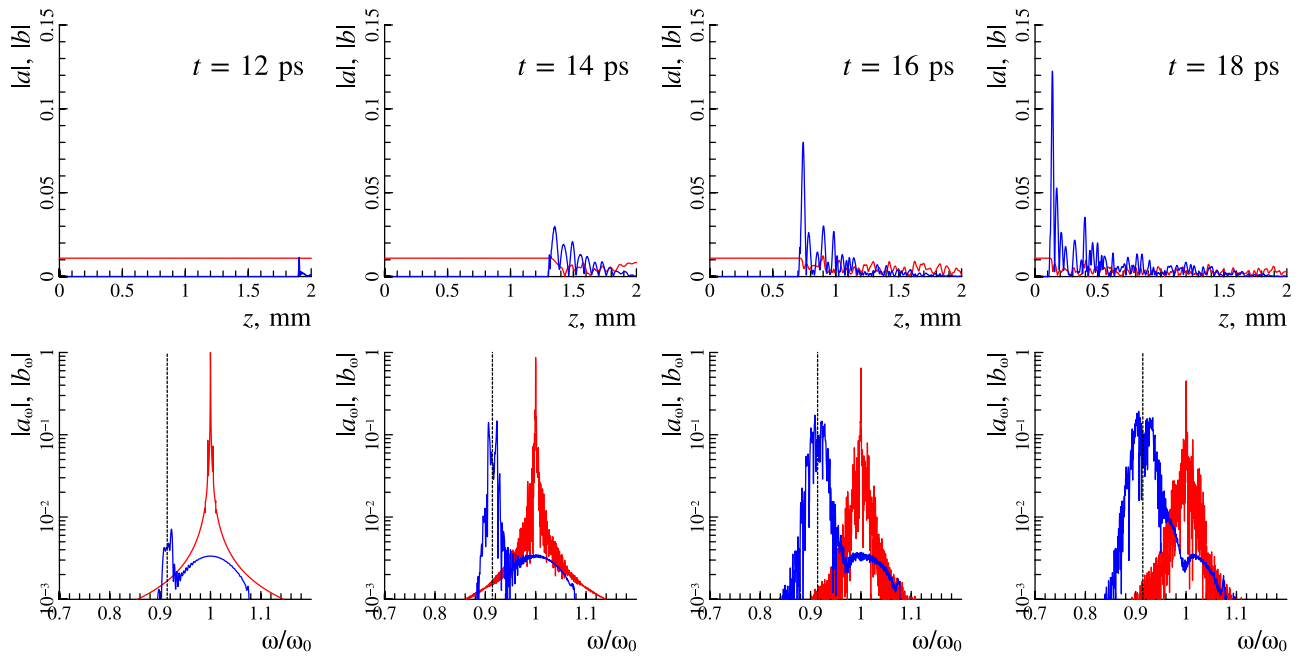
FIG. 4. Same as in Fig. 3 but for an inhomogeneous background plasma with density of the form (52) with $\delta N = 0.2$ and $L_\delta = 200\,\mu m$.

reported there is the solution for a delta-shaped pulse, which has *infinitely* broad spectrum), and the condition of efficient amplification is $\delta \omega_p \ll a\sqrt{\omega \omega_p}$. In other words, each given frequency must remain resonant up to the Raman growth rate, which is a natural measure of spectral broadening. In our simulations, this condition is not satisfied for *any* frequency. Thus, even linear amplification beyond the

three-wave resonance is not self-evident, let alone the non-linear regime.

The improved tolerance of BRA with respect to density inhomogeneities is interpreted as follows. At each given moment, BRA is most efficient for the part of the seed spectrum that satisfies the condition of the local Raman resonance [Eq. (45)]. This implies that different harmonics are
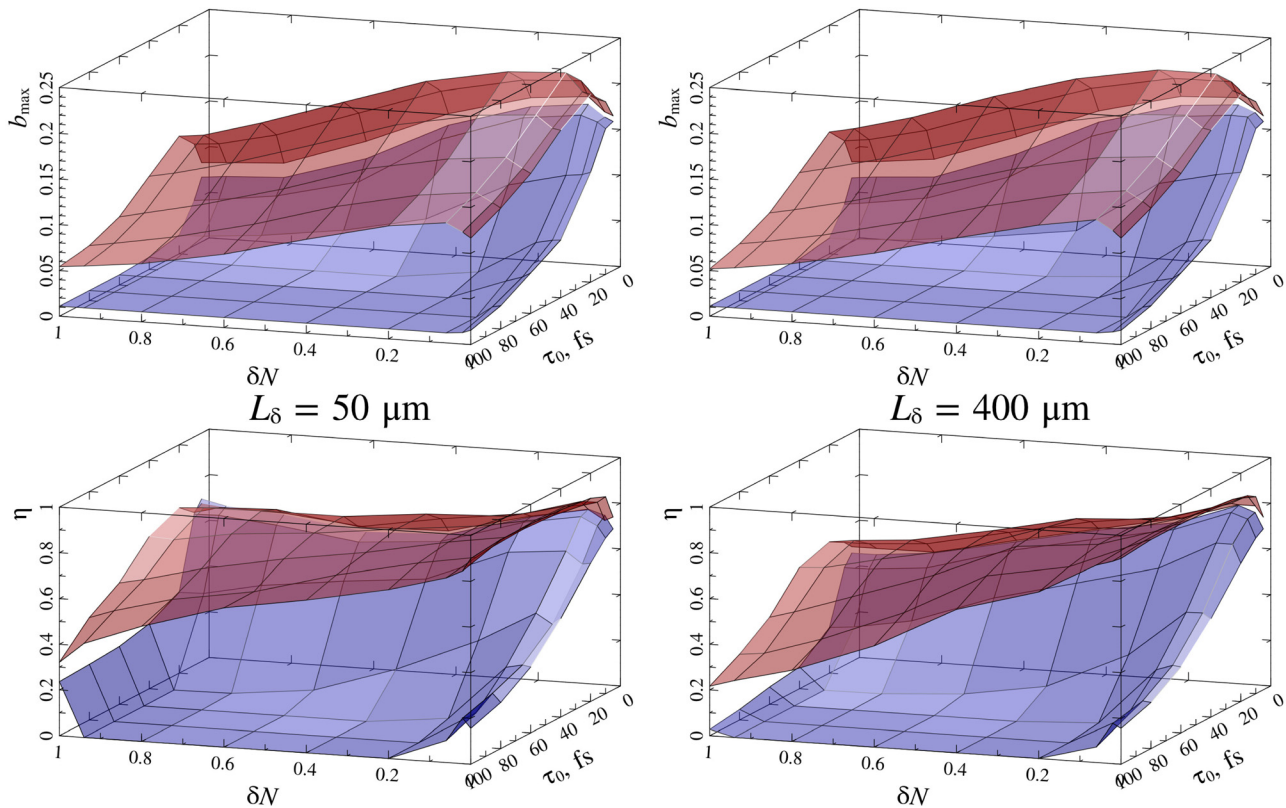

FIG. 5. Same as in Fig. 3 but for an inhomogeneous background plasma with density of the form (52) with various δN: left column—$L_\delta = 50\,\mu m$ and right column—$L_\delta = 400\,\mu m$.

amplified at different z. But their phases remain correlated near the seed front, so, there, the harmonics still can interfere constructively (albeit after a distance longer than that required to form the standard π pulse). This results in the amplification of the leading peak and, eventually, in pump depletion. But the coherence is largely lost at the tail of the seed, so the tail structure ends up being less regular (Fig. 4).

At larger δN, a larger amplification length is needed for this mechanism to be efficient. Thus, at a given amplification length, both b_{max} and η decrease accordingly. The effect is most dramatic for weak signals. Note also that BRA is most tolerant to smaller-scale inhomogeneities, for their influence is effectively averaged over the pulse trajectory. In contrast, larger-scale inhomogeneities cause linear transformations of the seed spectrum according to the standard equations of geometrical optics.[28] This makes it harder to satisfy the Raman-resonance condition; then, b_{max} and η decrease (Fig. 5).

V. CONCLUSIONS

To summarize, we proposed a reduced fluid model of Raman backscattering that describes BRA of pulses with duration comparable to or even smaller than the plasma period. Using our theoretical model, we numerically calculated the BRA efficiency for such pulses as a function of τ_0 and showed that it remains reasonably high up to $\tau_0 \approx 2\pi/\omega_p$. We also showed that using short seed pulses in BRA makes the amplification less sensitive to quasistatic inhomogeneities of the plasma density. Amplification can persist even when the density perturbations are large enough to violate the commonly known condition of resonant amplification.

The simplicity of our model allows us to state conclusively that the effects we identified in this paper are robustly of hydrodynamic origin. This provides a guidance to how BRA can be optimized, in the future, at the coarse level. Kinetic effects are the next level of complexity, so they can be studied separately.

ACKNOWLEDGMENTS

APPENDIX: THREE-WAVE MODEL

Here, we show that, in the limiting case when $\mathbf{a}$, $\mathbf{b}$, and f have sufficiently narrow spectra, Eqs. (40)–(43) lead to the traditional three-wave model of SRBS as in Ref. 1. In this limit, one can adopt $\hat{K}_{a,b} \approx -i/2$ and

$$\partial_z(\tilde{p}N_0) \approx 2i\tilde{p}N_0, \tag{A1}$$

$$\partial_z(\mathbf{a} \cdot \mathbf{b}^*) \approx 2i(\mathbf{a} \cdot \mathbf{b}^*), \tag{A2}$$

$$\partial_z^{-1} f \approx (2i)^{-1} f. \tag{A3}$$

Then,

$$(\partial_t + \partial_z)\mathbf{a} = -(i/2)\,\beta(N_0\mathbf{a} + \mathbf{b}f) + (i/2)\,\nabla_\perp^2\mathbf{a}, \tag{A4}$$

$$(\partial_t - \partial_z)\mathbf{b} = -(i/2)\,\beta(N_0\mathbf{b} + \mathbf{a}f^*) + (i/2)\,\nabla_\perp^2\mathbf{b}, \tag{A5}$$

$$\partial_t f + 2i\tilde{p}N_0 = 0, \tag{A6}$$

$$\partial_t\tilde{p} + 2i(\mathbf{a} \cdot \mathbf{b}^*) + \beta f/2 = 0. \tag{A7}$$

The latter pair of equations can be combined as follows:

$$\partial_t^2 f = -2iN_0\partial_t\tilde{p} = -4N_0(\mathbf{a} \cdot \mathbf{b}^*) - \beta N_0 f, \tag{A8}$$

or, equivalently,

$$\partial_t^2 f + \beta N_0 f = -4N_0(\mathbf{a} \cdot \mathbf{b}^*). \tag{A9}$$

This equation describes a driven oscillator with frequency $\Omega_p \doteq \sqrt{\beta N_0}$, which is just the local plasma frequency in dimensionless units. Since we have assumed that the spectrum of f is narrow, we can use

$$\partial_t^2 f \approx -\Omega_p^2 f - 2i\Omega_p(\partial_t + i\Omega_p)f. \tag{A10}$$

This gives

$$\partial_t f + i\Omega_p f = -\frac{2iN_0}{\Omega_p}\,(\mathbf{a} \cdot \mathbf{b}^*). \tag{A11}$$

Equations (A4), (A5), and (A11) form a complete set of equations describing a three-wave resonant interaction. Specifically, f is understood as the plasma wave that can be excited resonantly if the difference between the carrier frequencies of $\mathbf{a}$ and $\mathbf{b}$ equals the local plasma frequency.

Now let us measure t and z in units X and f in units iF, with X and F that satisfy

$$\frac{1}{2}\,XF\beta = 1, \quad \frac{2XN_0}{F\Omega_p} = 1, \tag{A12}$$

which is equivalent to

$$X = \frac{1}{\sqrt{\Omega_p}}, \quad F = \frac{2N_0}{\Omega_p^{3/2}}. \tag{A13}$$

In dimensional representation, this amounts to measuring coordinates in the units $c/\sqrt{\omega\omega_p}$ and the amplitude of density inhomogeneities in the units $2in(\omega_0/\omega_p)^2$ [i.e., the new f is nothing but $-eE_z/(mc\omega_p^2)$], where ω_p is the local plasma frequency. The corresponding equations are

$$(\partial_t + \partial_z)\mathbf{a} + (i/2)\,\Omega_p^2\mathbf{a} - (i/2)\,\nabla_\perp^2\mathbf{a} = \mathbf{b}f, \tag{A14}$$

$$(\partial_t - \partial_z)\mathbf{b} + (i/2)\,\Omega_p^2\mathbf{b} - (i/2)\,\nabla_\perp^2\mathbf{b} = -\mathbf{a}f^*, \tag{A15}$$

$$\partial_t f + i\Omega_p f = -\mathbf{a} \cdot \mathbf{b}^*, \tag{A16}$$

and, clearly, efficient interaction within this model is possible only under the condition (45).

In a homogeneous plasma, the terms containing Ω_p can be eliminated using a variable transformation, e.g.,

$$\mathbf{a} \rightarrow \mathbf{a}e^{-i\Omega_p(t-z)-i\Omega_p^2t/2}, \tag{A17}$$

$$\mathbf{b} \to \mathbf{b}e^{-i\Omega_p^2 t/2}, \quad f \to f e^{-i\Omega_p t}. \tag{A18}$$

Suppose also that diffraction is negligible. Then, the above equations are simplified down to

$$(\partial_t + \partial_z)\mathbf{a} = \mathbf{b}f, \quad (\partial_t - \partial_z)\mathbf{b} = -\mathbf{a}f^*, \quad \partial_t f = -\mathbf{a} \cdot \mathbf{b}^*.$$

Let us also introduce $\zeta \doteq z + t$ and assume $(\partial_t)_\zeta \ll (\partial_\zeta)_t$, as in Ref. 1. (The indexes denote the variables that are kept fixed at differentiation.) Then, one gets

$$2\partial_\zeta \mathbf{a} = \mathbf{b}f, \quad \partial_t \mathbf{b} = -\mathbf{a}f^*, \quad \partial_\zeta f = -\mathbf{a} \cdot \mathbf{b}^* \tag{A19}$$

[here, all fields are considered as functions of (t, ζ)], where we used $(\partial_t)_z = (\partial_t)_\zeta + (\partial_\zeta)_t$ and $(\partial_z)_t = (\partial_\zeta)_t$.

Notice also that Eqs. (A19) yield the Manley-Rowe relation $2|\mathbf{a}|^2 + |f|^2 = $ const. Assuming that f is initially zero, this leads to a useful estimate for the plasma wave amplitude: $f \sim a_0$ (here, a_0 is the amplitude of the unperturbed pump), or, in our original units,

$$f \sim Fa_0 \sim \frac{a_0}{\Omega_p^{3/2}} \sim \frac{a_0}{\beta^{3/4}}. \tag{A20}$$

[1]V. M. Malkin, G. Shvets, and N. J. Fisch, Phys. Rev. Lett. **82**, 4448 (1999).

[2]N. J. Fisch and V. M. Malkin, Phys. Plasmas **10**, 2056 (2003).

[3]V. M. Malkin, G. Shvets, and N. J. Fisch, Phys. Plasmas **7**, 2232 (2000).

[4]D. S. Clark and N. J. Fisch, Phys. Plasmas **10**, 3363 (2003).

[5]R. M. G. M. Trines, F. Fiuza, R. Bingham, R. A. Fonseca, L. O. Silva, R. A. Cairns, and P. A. Norreys, Nat. Phys. **7**, 87 (2011).

[6]V. M. Malkin and N. J. Fisch, Eur. Phys. J. Spec. Top. **223**, 1157 (2014).

[7]W. Cheng, Y. Avitzour, Y. Ping, S. Suckewer, N. J. Fisch, M. S. Hur, and J. S. Wurtele, Phys. Rev. Lett. **94**, 045003 (2005).

[8]Y. Ping, W. Cheng, S. Suckewer, D. S. Clark, and N. J. Fisch, Phys. Rev. Lett. **92**, 175007 (2004).

[9]N. A. Yampolsky and N. J. Fisch, Phys. Plasmas **18**, 056711 (2011).

[10]A. A. Solodov, V. M. Malkin, and N. J. Fisch, Phys. Plasmas **10**, 2540 (2003).

[11]L. Lancia, J.-R. Marquès, M. Nakatsutsumi, C. Riconda, S. Weber, S. Hüller, A. Mančić, P. Antici, V. T. Tikhonchuk, and A. Héron, Phys. Rev. Lett. **104**, 025001 (2010).

[12]L. Lancia, A. Giribono, L. Vassura, M. Chiaramello, C. Riconda, S. Weber, A. Castan, A. Chatelain, A. Frank, T. Gangolf, M. N. Quinn, J. Fuchs, and J.-R. Marquès, Phys. Rev. Lett. **116**, 075001 (2016).

[13]G. Lehmann and K. H. Spatschek, Phys. Plasmas **20**, 073112 (2013).

[14]G. Lehmann, K. H. Spatschek, and G. Sewell, Phys. Rev. E **87**, 063107 (2013).

[15]D. E. Ruiz and I. Y. Dodin, Phys. Lett. A **379**, 2623 (2015).

[16]Note that our a is twice the parameter a that is commonly used in literature. In particular, our $a = 1$ corresponds to the intensity about 4.94×10^{18} W/cm^2.

[17]I. Y. Dodin, V. I. Geyko, and N. J. Fisch, Phys. Plasmas **16**, 112101 (2009).

[18]I. Y. Dodin and N. J. Fisch, Phys. Rev. D **82**, 044044 (2010).

[19]C. Liu and I. Y. Dodin, Phys. Plasmas **22**, 082117 (2015).

[20]I. Y. Dodin, Fusion Sci. Technol. **65**, 54 (2014).

[21]For an application of the Lagrangian formulation to SRBS, see also P. Khain, L. Friedland, A. G. Shagalov, and J. S. Wurtele, Phys. Plasmas **19**, 072319 (2012).

[22]A. A. Balakin, G. M. Fraiman, N. J. Fisch, and V. M. Malkin, Phys. Plasmas **10**, 4856 (2003).

[23]M. S. Hur and J. S. Wurtele, Comput. Phys. Commun. **180**, 651 (2009).

[24]V. V. Lozhkarev, G. I. Freidman, V. N. Ginzburg, E. V. Katin, E. A. Khazanovm, A. V. Kirsanov, G. A. Luchinin, A. N. Mal'shakov, M. A. Martyanov, O. V. Palashov, A. K. Poteomkin, A. M. Sergeev, A. A. Shaykin, and I. V. Yakovlev, Laser Phys. Lett. **4**, 421 (2007).

[25]V. E. Fortov, *Extreme States of Matter: High Energy Density Physics*, 2nd ed. (Springer, New York, 2016).

[26]When the background density is homogeneous, one can always choose units such that $N_0 = 1$. Alternatively, replacing β with βN_0 in the denominator in Eq. (49) also leads to an exact dispersion relation at arbitrary N_0. However, when N_0 is inhomogeneous, one would have to specify how to interpret such $\hat{K}_{a,b}$, since N_0 and ∂_z do not commute in this case. We prefer to avoid such complications in the present paper for the sake of clarity.

[27]N. A. Yampolsky, V. M. Malkin, and N. J. Fisch, Phys. Rev. E **69**, 036401 (2004).

[28]T. H. Stix, *Waves in Plasmas* (AIP, New York, 1992).